JOURNAL OF GEOPHYSICAL RESEARCH, VOL. 93, NO. B9, PAGES 10,236–10,254, SEPTEMBER 10, 1988

Wrinkle Ridge Assemblages on the Terrestrial Planets

THOMAS R. WATTERS

Center for Earth and Planetary Studies, National Air and Space Museum
Smithsonian Institution, Washington, D.C.

The wrinkle ridge assemblage is a group of associated features that have been observed on the Moon, Mars, and Mercury. Members of the wrinkle ridge assemblage are classified as either arches or ridges based on morphology and ridges are subdivided into first-, second-, or third-order ridges on the basis of dimensions. The ridge assemblages described in this study are known to occur in mare basalts on the Moon and smooth plains units that may be volcanic in origin on Mars and Mercury. The structures that occur in the continental flood basalts of the Columbia Plateau in the northwestern United States are morphologically and dimensionally similar to features in the ridge assemblages on the terrestrial planets. The anticlinal ridges of the Columbia Plateau and many first-order ridges on the Moon, Mars, and Mercury are interpreted to be folds with reverse or thrust faulting developed as a result of buckling (flexure-fracture) or buckling as a consequence of reverse or thrust faulting (fracture-flexure). Estimates of the unit shortening across first-order ridges, using simple geometric forms to approximate the ridge morphology, are lower than those determined for the anticlines of the Columbia Plateau, where displacements are the results of folding and reverse to thrust faulting. Evidence of layer-parallel extension that often accompanies folds developed by fracture-flexure mechanisms (i.e., drape or fault-bend folds) is not found in the anticlinal ridges of the Columbia Plateau and has only been observed in one ridge on the Moon. A kinematic model involving buckling followed by reverse to thrust faulting (flexure-fracture) is favored for the origin of the anticlinal ridges of the Columbia Plateau and many of the first-order ridges on the Moon, Mars, and Mercury.

INTRODUCTION

Investigations of the surfaces of the terrestrial planets have revealed an association of features often collectively referred to as "wrinkle ridges," a term originally used in the description of lunar mare ridges. Mare ridges or wrinkle ridges have classically been described as consisting of a broad arch and an associated narrow ridge [*Storm*, 1972; *Bryan*, 1973; *Maxwell et al.*, 1975]. An analogous assemblage of features has been observed on Mercury and Mars. The ridges described in this study occur in lunar mare and in basins and on plains on Mars and Mercury. The regions where the ridges are found can be broadly divided into three physiographic settings: (1) basins, usually impact in origin that are subsequently filled by smooth plains material, (2) plateau plains, broad regions of smooth plains, and (3) intercrater plains, areas of smooth plains with limited areal extent. The origin of these ridges is not well understood but is clearly complex. Models for the origin of the ridges involve purely volcanic and purely tectonic mechanisms, some with elements of both.

The purpose of this study is (1) to investigate the morphological and dimensional similarities of the arches and ridges observed on the terrestrial planets, (2) to establish a basis for a structural interpretation of these features using structures on the Columbia Plateau as analogs, (3) to estimate the strain across the ridges and to compare this with existing estimates for lunar mare ridges and the anticlinal ridges of the Columbia Plateau, and (4) to discuss the importance of reverse or thrust faulting in the origin of the ridges.

Paper number 7B4012.
0148-0227/88/007B-4012$05.00

MORPHOLOGY

Wrinkle ridge assemblages on the Moon, Mars, and Mercury consist of two distinct morphologic features generally described as arches and ridges. Arches are broad, gently sloping, curvilinear topographic rises that are commonly asymmetric in profile [*Strom*, 1972; *Bryan*, 1973]. Ridges are long, relatively narrow, segmented features that are commonly strongly asymmetric in cross section. The sense of the asymmetry may change either along strike or from one ridge segment to the next, and segments often occur in en echelon arrangements. In wrinkle ridge assemblages in mare basins the ridge is often superposed on the arch [*Strom*, 1972; *Bryan*, 1973; *Maxwell et al.*, 1975]. In addition to this ridge-arch association, there is evidence of smaller secondary ridges that occur on or near larger primary ridges.

In an effort to characterize quantitatively the morphology and dimensions of the features encompassed by the term wrinkle ridge, the approximate height and width of 185 structures were determined from topographic maps, images, and shadow measurements (see the appendix). Arches and ridges can be readily distinguished on the basis of dimension (Figure 1). The size distribution of the ridge data forms a continuum but with discernible clusterings. The clusters within the ridge data fall over 3 orders of magnitude in scale (Figure 1). Thus the ridges within these clusters are described as first-, second-, and third-order ridges. The arch data define a separate field from the ridge data (Figure 1). Regression lines fit to the ridge and arch data have correlation coefficient (r) of 0.81 and 0.78, respectively (Figure 1). The regression lines can be roughly approximated by a width to height (w/h) ratio of 10 for the ridges and 70 for the arches. The classification described above is offered as a means of facilitating the description and analysis of the members of the wrinkle ridge assemblage on the Moon, Mars, and Mercury and to allow comparisons with potential terres-

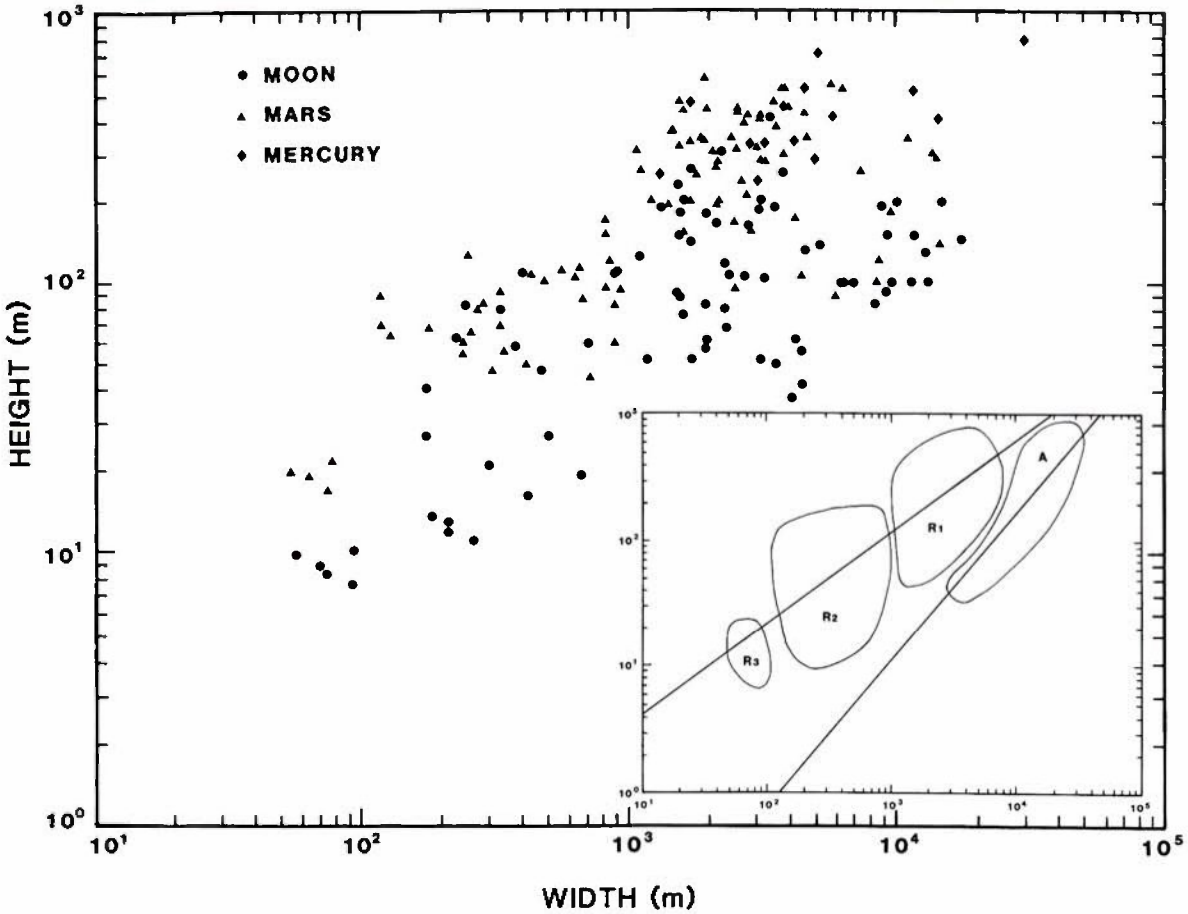

Fig. 1. Log-log plot of height versus width of 185 features in ridge assemblages on the Moon, Mars, and Mercury. Arches (A), first-order ridges (R_1), second-order ridges (R_2), and third-order ridges (R_3) form discernible clusters. The regression line for the ridge data (slope log $m = 0.72$, intercept log $c = -0.097$) and arch data (log $m = 1.17$, log $c = -2.47$) can be roughly approximated by w/h ratio of 10 and 70, respectively. The fields shown enclose all the observations of a given feature.

trial analogs. The morphology, dimensions, and spatial relationships of the arches and ridges examined in this study are described in the following sections.

Moon

Lunar mare ridges are probably the best described of those observed on the terrestrial planets and are found in nearly all lunar maria [*Head*, 1976]. The mare wrinkle ridge assemblages typically occur both radial to and concentric with the centers of circular mare basins [*Bryan*, 1973; *Maxwell et al.*, 1975]. Arches are broad, gently sloping topographic rises (Figures 2 and 3*a* and Table 1), often only distinguishable in low sun angle images [*Strom*, 1972; *Bryan*, 1973; *Maxwell et al.*, 1975]. The first-order mare ridges are narrow relative to arches, sinuous, and often strongly asymmetric (Figures 1 and 3*b* and Table 1). They are usually segmented, occurring in en echelon arrangement [see *Tija*, 1970]. Many of the first-order ridges are associated with arches (Figures 2 and 3*a*). In some cases the ridges are superposed on the associated arch [*Strom*, 1972; *Maxwell et al.*, 1975]. Second-order mare ridges are sharp, narrow prominences that are very similar in morphology to the first-order ridges (Figure 2 and Table 1) and commonly flank or cap the larger ridges (Figures 3*b* and 4). Third-order ridges are similar in morphology to first- and second-order ridges, commonly cap or flank the larger features (Figure 4) and can only be easily resolved in Apollo metric camera and panoramic camera images. *Scott* [1973] describes several of these small-scale ridges in the Taurus-Littrow region that occur independently of larger structures in the wrinkle ridge assemblage.

Mars

The Mariner 9 and Viking missions to Mars revealed the greatest population of lunarlike ridges observed on a terrestrial planet. The Martian ridges include the same types of features as their lunar counterparts (see also *Lucchitta and Klockenbrink* [1981]). Martian arches and ridges are practically indistinguishable in morphology from their lunar analogs (Figure 5 and Table 2). As is often the case for mare ridge assemblages, some first-order Martian ridges are associated with arches, either superposed on or flanking the broader features (Figure 5) [*Lucchitta and Klockenbrink*, 1981]. Second-order ridges are also present in the Martian ridge assemblages but are only clearly distinguishable in the high-resolution Viking orbiter images (< 100 m/pixel) (Figure 6*a* and Table 2). Like their lunar analogs, second-order Martian ridges often cap or flank first-order ridges. Third-order ridges are also associated with the larger ridges but can only be clearly resolved

Fig. 2. Mare ridge assemblages in Oceanus Procellarum, near the northwestern edge of the Aristarchus Plateau (lower right). The ridge assemblage consists of (A) arches, (R_1) first-order ridges, (R_2) second-order ridges, and (R_3) third-order ridges (see Figure 4). An arch may be capped or flanked by a ridge. First-order ridges, in turn, may be flanked by second-order ridges (Apollo 15 Metric Camera AS15-2486).

in very high resolution (~10 m/pixel) Viking orbiter images (Figure 6*b* and Table 2).

Mercury

Mariner 10 revealed morphologically and dimensionally similar structures to the lunar and Martian ridges on the surface of Mercury (Figure 7 and Table 3). Arches and first-order ridges are the only members in the wrinkle ridge assemblage observed on Mercury [*Strom et al.*, 1975; *Maxwell and Gifford*, 1980]. Second- and third-order ridges may be present but cannot be resolved in the medium- to low-resolution (showing details from 1200 to 200 m) Mariner 10 images. Unlike some of their counterparts on the Moon and Mars, none of the observed Mercurian ridges are superposed on adjacent arches [*Strom et al.*, 1975; *Maxwell and Gifford*, 1980].

Venus

The Venera 15 and 16 spacecraft have returned radar images of the surface of Venus that show evidence of long, narrow relatively high-relief features on the presumed volcanic plains near Metis Regio (a domal feature near 70°N, 105°E). These features are interpreted to be similar to lunar ridges.

TABLE 1. Dimensions of Features in Ridge Assemblages on the Moon

Feature	$\bar{X}_w$	s_w	X_{max}–X_{min}	$\bar{X}_h$, m	s_h, m	X_{max}–X_{min}, m	n
Arches	8.6 km	3.7 km	17.5–3.1 km	107	46	200–37	21
First-order ridges	2.3 km	0.9 km	5.2–1.2 km	145	79	408–45	34
Second-order ridges	401 m	211 m	900–174 m	49	33	110–11	19
Third-order ridges	77 m	11 m	94–57 m	9	0.7	10–8	5

$\bar{X}_w$, mean width; $\bar{X}_h$ mean height; s, standard deviation; range, X_{max}–X_{min}; and n, number of features. Measurements were made from Lunar Topographic Orthophotomaps, Apollo Metric Camera and Panoramic Camera images (see the appendix).

However, the resolution of the Venera radar images is not sufficient to allow a detailed morphologic comparison with the ridge assemblages on the other terrestrial planets.

LITHOLOGY

The common association between mare ridges, mare basins, and mare basalts on the Moon has led some workers to suggest a genetic relation between the basins and the origin of the features [see *Strom*, 1972; *Bryan*, 1973]. The presence of analogous ridges on certain plains units on Mars and Mercury has been used as indirect evidence to argue a volcanic origin for the material. Inferring the lithology using such criteria is currently the subject of some debate. Thus the question of what is known or inferred about the lithology of the material in which these features commonly occur is of some importance.

Moon

Samples of the mare rock returned from Apollo 11, 12, 15, and 17 established that the mare basins are filled with basalt. Evidence of lava flows into the mare basins [*Bryan*, 1973; *Schaber*, 1973*a*, *b*; *Schaber et al.*, 1976; *Maxwell*, 1978] suggest that the mare ridge assemblages occur in a multilayer basalt sequence.

Structures that occur in the lunar highlands or extend from the mare into the highlands have been described by *Howard and Muehlberger* [1973], *Lucchitta* [1976], *Binder* [1982], *Binder and Gunga* [1985], and *Raitala* [1984]. The assemblage of features described by *Lucchitta* [1976] as "mare-ridge, highland-scarp systems" occurs in the Taurus-Littrow of Mare Serenitatis (Lee Lincoln scarp) [*Howard and Muehlberger*, 1973; *Lucchitta*, 1976] and in western Serenitatis (West Serenitatis scarp) [*Lucchitta*, 1976]. The Lee Lincoln and West Serenitatis scarps offset the mare surface by as much as 100 m [*Lucchitta*, 1976], are capped by first-order ridges, and flanked and crosscut by second-order ridges [see *Howard and Muehlberger*, 1973, Figure 31-37]. Where the scarps extend into the highlands, a distinct change in the assemblage of features and the morphology of the scarps occurs. In the highlands the scarps are lobate, smooth, and segmented with a maximum height of 30 m [*Lucchitta*, 1976] [see *Howard and Muehlberger*, 1973, Figure 31-33; *Lucchitta*, 1976, Figures 2 and 8]. These highland scarps are morphologically distinct from any

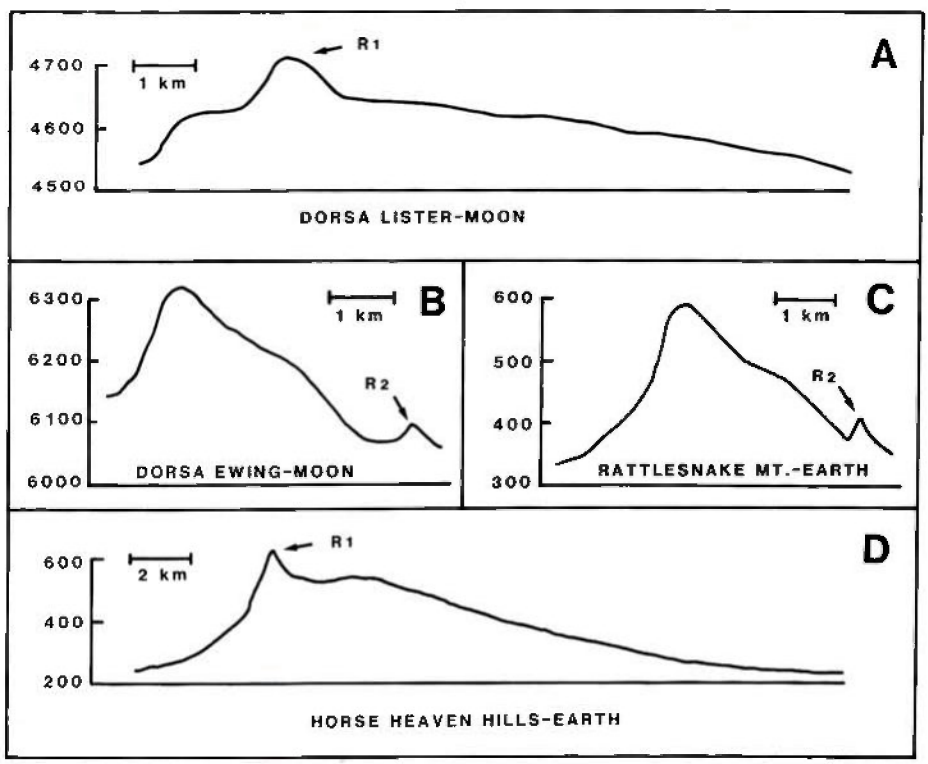

Fig. 3. Topographic cross sections of first and second-order ridges and arches on the Moon and analogous structures on the Columbia Plateau. Arches in Figures 3*a* and 3*d* are broad gently sloping rises that may be capped or flanked by ridges (R_1). Ridges in Figures 3*b* and 3*c* are relatively narrow and asymmetric. Second-order ridges (R_2) often flank the larger first-order ridge. Vertical scales are in meters.

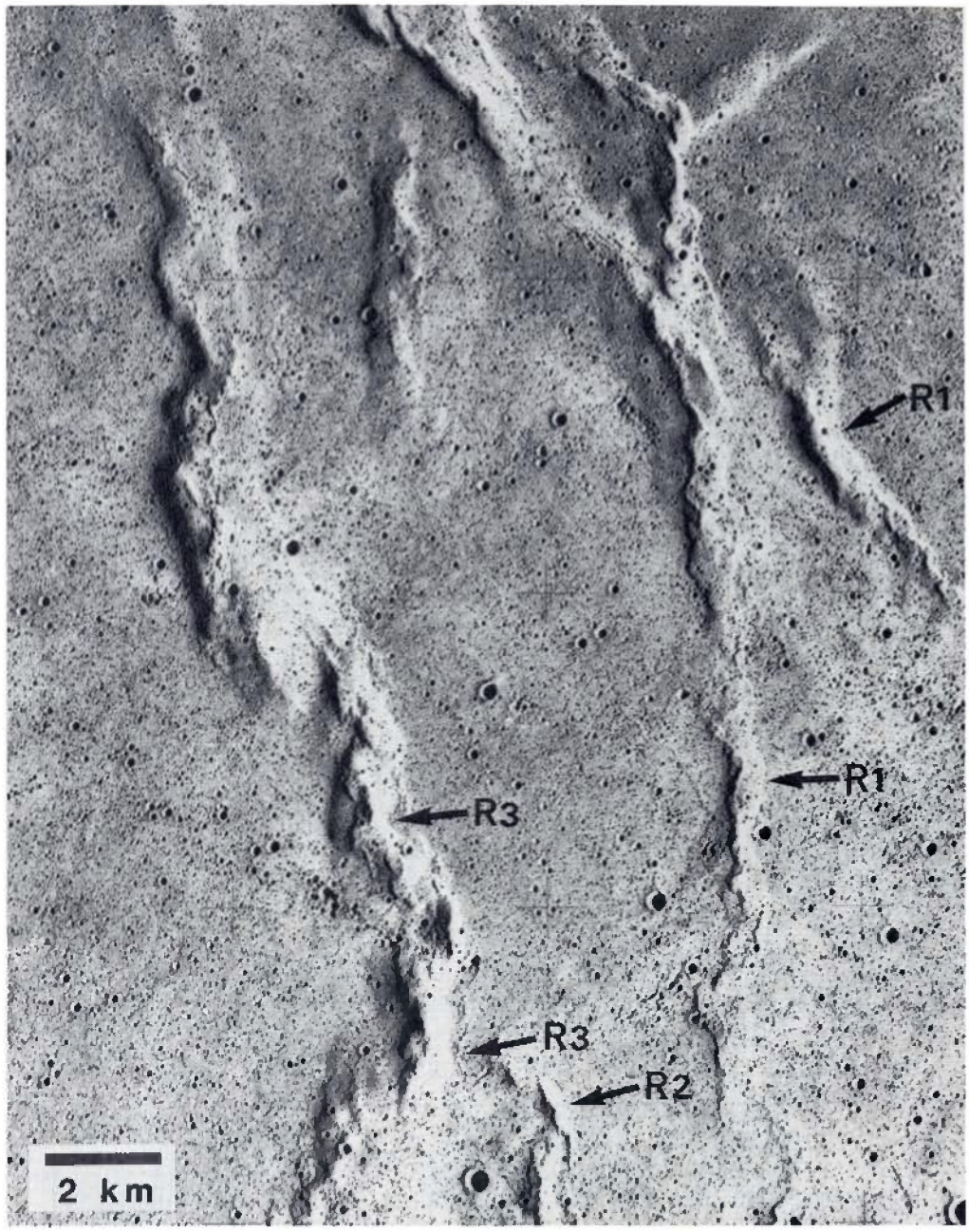

Fig. 4. Enlargement of a portion of Figure 2 (Oceanus Procellarum). Second-order (R_2) and third-order ridges (R_3) flanking larger first-order ridges (R_1) (Apollo Metric Camera AS15-2486).

of the features in the mare ridge assemblage. This is also true of the highland scarp near Fra Mauro [*Raitala*, 1984] [see Apollo Metric Camera frame AS14-70-9818] and those near Mendeleev and on the floor of Mandel'shtam [*Binder*, 1982, Figures 7 and 8; *Binder and Gunga*, 1985, Figure 6].

Mars

The ridge assemblages on Mars are observed in smooth plains material that occurs in a variety of settings: (1) the Tharsis Plateau (i.e., Coprates, Lunae Planum and Tempe Terra), (2) the Amazonis and Chryse lowlands, (3) the plains of Syrtis Major, Hesperia Planum, and Malea Planum, (4) in basins such as Schiaparelli, Huygens, Copernicus, and Newton, (5) intercrater plains of Phaethontis, Memnonia, and Eridania and north and east of the Schiaparelli basin, and (6) within the Ascraeus Mons and Olympus Mons calderas.

The plateau ridges of Coprates, Lunae Planum, and Tempe Terra; the intercrater plains ridges of Phaethontis and Memnonia; and the ridge in the Chryse and Amazonis lowlands are all associated with the Tharsis Plateau ridge system [*Watters and Maxwell*, 1986]. These ridged plains units are associated with the largest volcanic center on the planet [*Scott and Tanaka*, 1986; *Basaltic Volcanism Study Project* (BVSP), 1981]. The ridged plains of Sytris Major (10°N, 70°E), Hesperia (20°S, 110°E), and Melea Planum (60°S, 45°E) are also associated with major volcanic centers [*Scott and Carr*, 1978; *Carr et al.*, 1977; *Schaber*, 1982]. The Schiaparelli (3°S, 16°E), Huygens (15°S, 46°E), Copernicus (50°S, 169°W), and Newton

Fig. 5. Ridge assemblage of the Coprates region of the Tharsis Plateau of Mars. Martian arches (A) and first-order ridges (R_1) are very similar morphologically to their lunar analogs (Viking orbiter frame 608A45).

(158°W, 41°S) basins are very similar in morphology and origin to lunar mare basins [*Maxwell and Gifford*, 1981; *Mouginis-Mark et al.*, 1981]. The age of the smooth plains varies greatly from the ancient Noachian plains of Malea Planum to perhaps the youngest in the Olympus Mons caldera.

Based on photogeologic evidence of volcanic landforms (i.e., flow fronts) and comparisons with terrestrial flood basalt provinces and lunar maria much of the smooth plains material on Mars has been interpreted to be the results of flood volcanism [*Scott and Carr*, 1978; *Greeley et al.*, 1977; *BVSP*, 1981; *Mouginis-Mark et al.*, 1981; *Lucchitta and Klockenbrink*, 1981; *Scott and Tanaka*, 1986]. Although there is no direct evidence to support such an interpretation and alternative interpretations (i.e., the possible existence of sedimentary material) must be considered, a volcanic origin for much of the smooth plains material is not an unreasonable hypothesis. None of the features in the Martian wrinkle ridge assemblage, as described in this study, have been observed in either the heavily cratered uplands material (highlands) or extending from smooth plains into adjacent uplands material. *Lucchitta and Klockenbrink* [1981] observe that ridges on Mars do not occur on (1) thick crater ejecta, (2) what appears to be soft, possibly sedimentary material (i.e., the floor deposits of Valles Marineris), and (3) rough topography or fractured plains.

Mercury

Ridges on Mercury are restricted to three units mapped by *Strom et al.* [1975] as smooth plains, hummocky plains, and intercrater plains. Nearly all the ridges are observed in the

TABLE 2. Dimensions of Features in Ridge Assemblages on Mars

Feature	$\bar{X}_w$	s_w	X_{max}–X_{min}	$\bar{X}_h$, m	s_h, m	X_{max}–X_{min}, m	n
Arches	8.9 km	3.8 km	14.4–2.2 km	171	100	499–89	9
First-order ridges	2.7 km	1.1 km	6.3–1.1 km	332	117	571–95	50
Second-order ridges	481 m	252 m	932–118 m	87	29	173–45	29
Third-order ridges	67 m	7 m	78–54 m	20	2	24–17	4

$\bar{X}_W$, mean width; $\bar{X}_h$ mean height; s, standard deviation; range, X_{max}–X_{min}; and n, number of features. Measurements were made from Viking orbiter images (see the appendix).

smooth plains units [see *Strom et al.*, 1975, Figure 20] which occur both within and external to large basins and within large craters. The largest expanse of smooth plains material occurs in the Caloris Basin (35°N, 5°W) and Tir (3°N, 5°E), Budh (20°N, 30°E), and Borealis Planitiae (70°N, 80°W).

The origin of the smooth plains units on Mercury has been the subject of some controversy. Two hypotheses have been put forth: (1) the smooth plains are the result of flood volcanism [*Strom et al.*, 1975; *Trask and Strom*, 1976], and (2) they are the result of impact ejecta [*Wilhelms*, 1976; *Oberbeck et al.*, 1977]. An unequivocal case for a volcanic origin cannot be made because of the lack of photogeologic evidence of volcanic landforms (i.e., flow fronts, vents) [*Wilhelms*, 1976]. Arguments against the smooth plains being composed of ejecta are based on (1) large areal extent of smooth plains and (2) lack of smooth plains surrounding basins of comparable age to Caloris [*Trask and Strom*, 1976]. *Malin* [1978] observes that the clearest photogeologic evidence of volcanic landforms on the Moon (using Earth-based telescopic images of similar resolution to Mariner 10 images) are lost in images

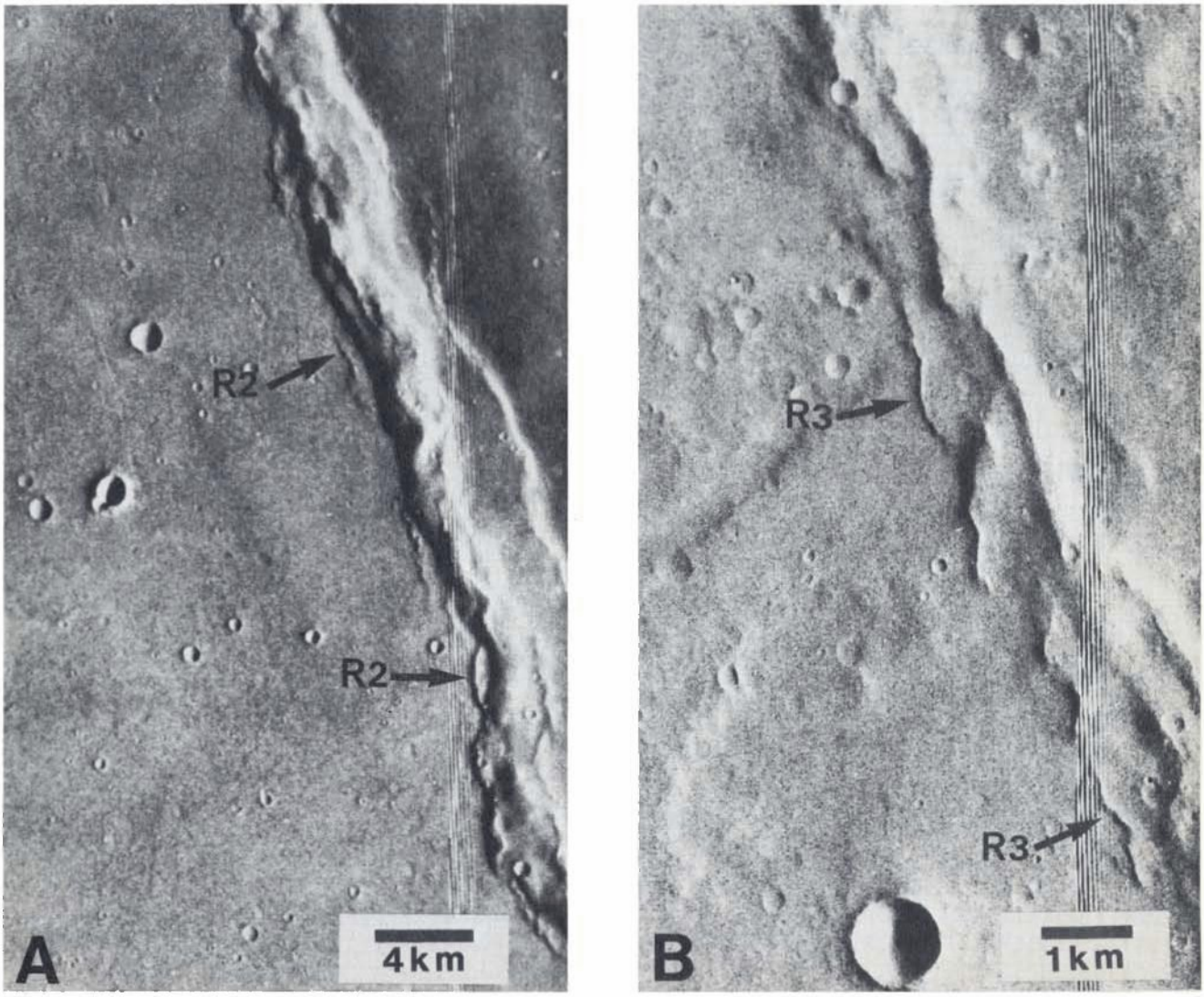

Fig. 6. Martian second- and third-order ridges. (*a*) Second-order ridges (R_2) and (*b*) third-order ridges (R_3) flanking larger first-order ridges (Viking orbiter frame 664A18, 813A06).

Fig. 7. Ridges in the Caloris Basin of Mercury. First-order ridges (R_1) and arches are the only members of the ridge assemblage that have been observed. Second- and third-order ridges may exist but cannot be resolved in Mariner 10 imagery (Mariner 10, FDS 126).

with incident angles $>10°$. However, *Malin* [1978] describes two domelike landforms (one along the Discovery Scarp near 50°S, 35°W, and the other in the south polar region near 64°S, 152°W) similar to those observed on the Moon as possible direct evidence of Mercurian volcanism. In addition, the presence of a magnetic field indicating that Mercury may have a partially molten metallic core supports arguments for volcanism on the planet [*BVSP*, 1981].

Hummocky plains units occur adjacent to the Caloris basin and are characterized by low scattered hills surrounded by smooth plains material [*Trask and Guest*, 1975]. In places, the contact between hummocky plains units and smooth plains material is gradational. *Trask and Guest* [1975] and *Strom et al.* [1975] suggest that the hummocky plains are a facies of the Caloris basin ejecta and upon emplacement contained a large component of molten materials. Most of the few ridges that occur in the hummocky plains extend into or from adjacent smooth plains units commonly where the contact between the two is gradational. As is the case on the Moon and Mars, wrinkle ridge assemblage structures are not observed in the heavily cratered upland terrain. In contrast to the ridges, lobate scarps that are similar in morphology to lunar highland scarps commonly cross a number of different geologic units [*Strom et al.*, 1975]. Many of these scarps, particularly the Discovery Scarp, are interpreted to be the result of reverse or thrust faulting [*Strom et al.*, 1975].

TABLE 3. Dimensions of Features in Ridge Assemblages on Mercury

Feature	$\bar{X}_w$, km	s_w, km	X_{max}–X_{min}, km	$\bar{X}_h$, m	s_h, m	X_{max}–X_{min}, m	n
Arches	18.6	6.6	30.0–11.5	583	117	782–447	3
First-order ridges	3.7	1.2	5.7–1.3	393	120	700–241	11

$\bar{X}_w$, mean width; $\bar{X}_h$ mean height; s, standard deviation; range, X_{max}–X_{min}; and n, number of features. Measurements were made from Viking orbiter images (see the appendix).

TERRESTRIAL ANALOGS

The common occurrence of ridges on the Moon, Mercury, and Mars has led to many attempts to locate terrestrial analogs to these structures. *Greeley and Spudis* [1978] suggest that terrestrial analogs for ridges wrinkle occur on the western Columbia Plateau (see also *Lucchitta and Klockenbrink* [1981], *Watters and Maxwell* [1985*a*], and *Plescia and Golombek* [1986]). The Columbia Plateau represents one of the largest continental flood basalt regions on the Earth, with a total areal extent of the order of 2×10^5 km^2 [*Tolan et al.*, 1987].

In the Yakima Fold Belt the multilayered basalts have been deformed into a series of sinuous, segmented, and en echelon anticlinal ridges (Figure 8). The anticlinal ridges are dimensionally similar to the first-order ridges of the wrinkle ridge assemblage (Figure 9 and Table 4). The Yakima folds (as they are commonly termed) are asymmetric in cross section, commonly consisting of a short, steeply dipping northern limb and a longer gently sloping southern limb (Figure 3*c*). Like first-order ridges on the terrestrial planets, the sense of the asymmetry may change from one segment to the next or along strike within a given segment. High-angle faults may separate ridge segments of opposite fold geometry [*Reidel*, 1978, 1984; *Fecht*, 1978; *Bentley et al.*, 1980]. The anticlines are separated by broad, flat-bottomed synclines that are largely undeformed [*Price*, 1982; *Reidel et al.*, 1984; *Reidel*, 1984]. Associated with the flanks of the vergent side of the anticlines are high-angle reverse to thrust faults that generally strike parallel to fold axes [see *Reidel et al.*, 1984].

In addition to the anticlinal ridges, smaller secondary folds with fold axes that trend subparallel to oblique to the larger anticlinal ridges are observed in the Yakima Fold Belt [*Reidel*, 1984, also personal communication, 1987]. These structures commonly occur either flanking or adjacent to the anticlinal ridges (Figure 10 and Table 4) and are similar in dimension and morphology to the second-order ridges observed on the Moon (Figures 9 and 3*c*) and Mars. Broad rises, similar in morphology and dimension to planetary arches, are associated with the Horse Heaven Hills ridge and the Rattlesnake Hills ridge (Figures 9 and 3*d* and Table 4). Nothing analogous to third-order ridges has been observed, but features of this scale, if they existed, may have been quickly lost to erosion.

The anticlinal ridges of the Columbia Plateau occur in a multilayered sequence of theoleiitic basalts erupted from early to late Miocene from linear vents [*Waters*, 1961]. The basalts reach a thickness in excess of 3 km in the Pasco Basin [*Reidel et al.*, 1982]. The greatest volumes of the Columbia River Basalt Group (CRBG) (Imnaha and Grande Ronde basalts) were emplaced during early Miocene. The upper sequence of the CRBG, made up of the Wanapum and Saddle Mountains basalts, contains a number of interbeds composed of volcanoclastic sediments [see *Reidel and Fecht*, 1987]. Individual flows of the CRBG range in thickness from 10 to 30 m and some can be traced for 200 km.

The areal extent of the Columbia River basalts is similar to that of the Eratosthenian flood basalts in Mare Imbrium [*Schaber*, 1973*b*]. Although the volume of the CRBG is estimated to be about 10–20 times greater than that of the lunar Eratosthenian basalts, the average flow heights in the Imbrium basin are from 1.5 to 1.8 times that of flows of the CRBG with similar flow lengths [*Schaber*, 1973*b*].

The anticlinal ridges of the Columbia Plateau are periodically spaced [*Watters*, 1987]. Periodic spacing of ridges is apparent on the ridged plains of the Tharsis Plateau [*Saunders and Gregory*, 1980; *Watters*, 1987], Hesperia Planum, and Syrtis Major on Mars and in basins on the Moon [see *Maxwell et al.*, 1975], Mercury [see *Maxwell and Gifford*, 1980], and Mars [see *Mouginis-Mark et al.*, 1981; *Maxwell and Gifford*, 1981]. Thus, based on similarities in morphology, dimension, and spatial relationship, the Yakima folds of the Columbia Plateau appear to be good terrestrial analogs to first-order ridges on the Moon, Mars, and Mercury. The smaller secondary folds associated with the anticlines are analogous to second-order ridges and the broad rises are possibly analogous to arches.

In a recent paper, *Plescia and Golombek* [1986] propose a number of structures, in addition to the anticlinal ridges of the Columbia Plateau, as terrestrial analogs to planetary wrinkle ridges. These features occur in a variety of different materials (i.e., soils, asphalt, sedimentary rocks) and range in scale from centimeters to kilometers. Of the structures suggested (other than the Columbia ridges), two are comparable in scale to the planetary features described in this study: (1) the Buena Vista Hills in western San Joaquin Valley, and (2) the Sera el Maarouf anticline in Algeria. The Buena Vista Hills are the surface expression of a series of anticlines formed in Miocene to Pleistocene sedimentary rocks and sediments (maximum relief ~180 m) resulting from stresses related to diffuse coupling movement along the San Andreas fault [*Harding*, 1976]. The Sera el Maarouf anticline (maximum relief ~200 m) occurs in Miocene and Pliocene marls and sandstones [*Yielding et al.*, 1981; *Philip and Meghraoui*, 1983]. The Sera el Maarouf anticline and the Buena Vista Hills are both folds associated with thrust faults [*Yielding et al.*, 1981; *Philip and Meghraoui*, 1983; *Harding*, 1976]. These structures as well as other similar features suggested by *Plescia and Golombek* [1986] may also serve as analogs to the ridges on the terrestrial planets. Because the wrinkle ridge assemblages on the Moon (described in this study) and the anticlinal ridges of the Columbia Plateau are also known to occur in basalts, it is tempting to speculate that these structures are particular to the deformation of basalt or basaltlike material. *Plescia and Golombek* [1986] argue against such an association based on the great variety of material in which their proposed analogs occur. Ultimately, the question of lithology of the material may be secondary to the question of the mechanical properties of the material. The anticlinal ridges of the Columbia Plateau, as well as many of the analogs proposed by *Plescia and Golombek* [1986] (particularly those mentioned above) occur in layered materials. If the material is mechanically anisotropic under conditions of deformation, the nature and scale of the anisotropy will greatly influence the style of deformation [*Donath*, 1962; *Donath and Parker*, 1964; *Ramsay*, 1967]. Thus, even though it is likely that the wrinkle ridge assemblages on Mars and Mercury (described in this study) occur in "basaltlike" material, it is not necessary.

INTERPRETATION OF RIDGES

Moon, Mars, and Mercury

The interpretation of ridges on the Moon, Mars, and Mercury is based on photogeologic and remote sensing studies and limited field work on the Moon. Lunar mare ridges have been interpreted to be the results of (1) intrusive volcanism [*Whitaker*, 1966; *Strom*, 1972], (2) extrusive volcanism [*Young et al.*, 1973; *Hodges*, 1973], (3) tectonic deformation [*Bryan*, 1973; *Schaber*, 1973*a*, *b*; *Howard and Muehlberger*, 1973;

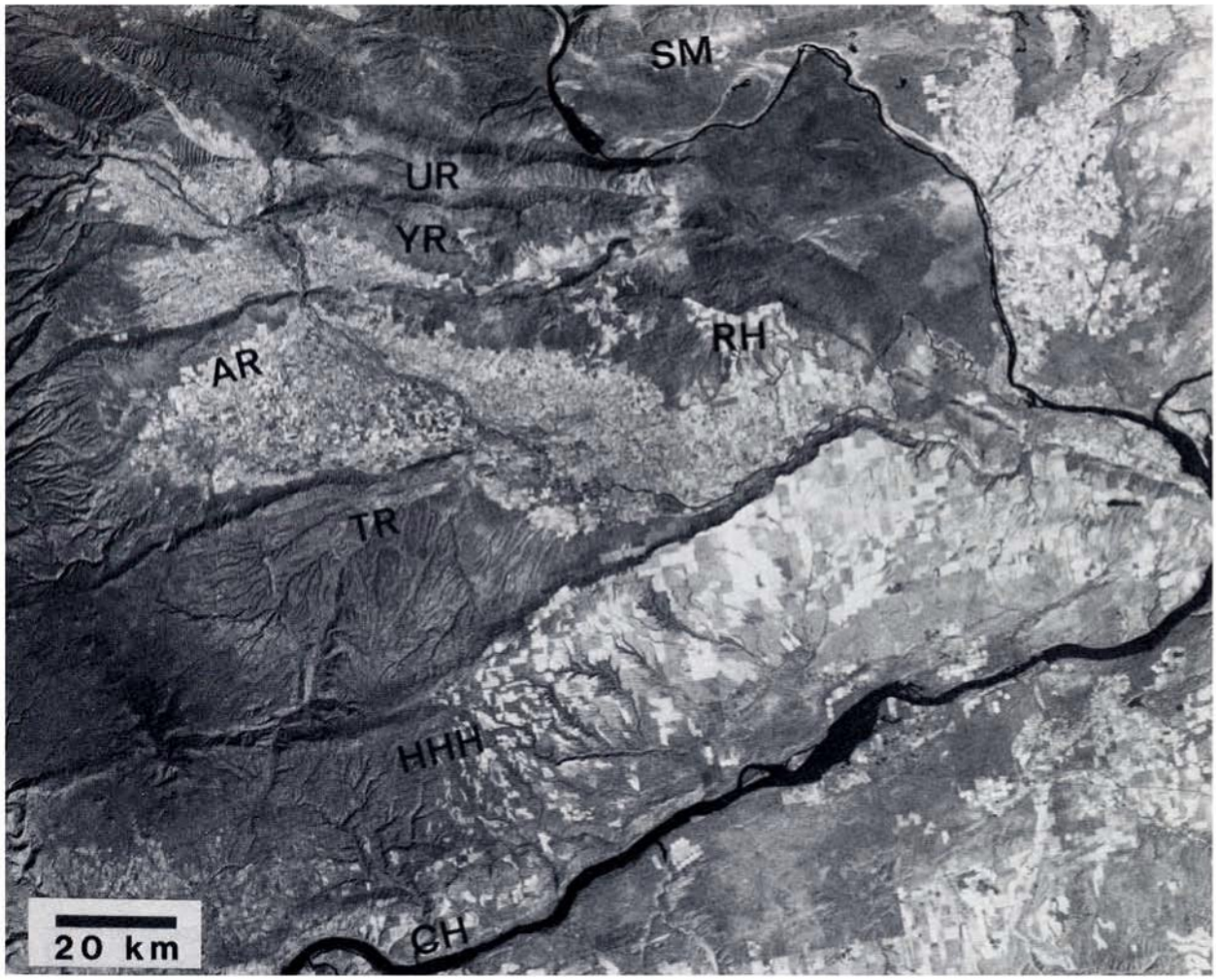

Fig. 8. Anticlinal ridges of the western Columbia Plateau. The ridges in the portion of the Yakima Fold Belt subprovince shown are the Columbia Hills (CH), Horse Heaven Hills (HHH), Toppenish Ridge (TR), Ahtanum Ridge (AR), Yakima Ridge (YR), Umtanum Ridge (UR), Saddle Mountains (SM), and Rattlesnake Ridge (RR) (Landsat 4, frame ID 4009518173).

Muehlberger, 1974; *Lucchitta*, 1976, 1977; *Maxwell*, 1978; *Sharpton and Head*, 1981, 1982], and (4) a combination of volcanic and tectonic mechanisms [*Tjia*, 1970; *Hartman and Wood*, 1971; *Colten et al.*, 1972]. The various hypotheses result largely from different interpretations of the morphology of the ridges. The most convincing support for a structural interpretation of mare ridges is the subsurface information provided by the Apollo Lunar Sounder Experiment (ALSE) data [*Peeples et al.*, 1978; *Maxwell and Phillips*, 1978]. ALSE data over a mare ridge assemblage in southeastern Serenitatis show evidence of thinning of a mare unit (sequence of flows) on apparent structural relief [*Maxwell*, 1978].

Based largely on a strong morphologic similarity to mare ridges, ridge assemblages on Mars have also been interpreted as either volcanic [*Greeley et al.*, 1977] or tectonic [*Lucchitta and Klockenbrink*, 1981] features. The ridges on the Tharsis Plateau are generally interpreted to be tectonic in origin based on morphology, crosscutting relationships with fractures and their spatial relationships within the ridge system [*Saunders and Gregory*, 1980; *Saunders et al.*, 1981; *Maxwell*, 1982; *Watters and Maxwell*, 1983, 1985*b*, *c*, 1986]. Ridges on Mercury are also generally interpreted as structural features on the basis of lunar analogs [*Strom et al.*, 1975; *Wilhelms*, 1976; *Maxwell and Gifford*, 1980].

Terrestrial Analogs

Fortunately, terrestrial analogs are almost always more accessible than their planetary counterparts. This is certainly the case for the anticlinal ridges of the Columbia Plateau. In the field it is clear that these structures involve buckling of a multilayered sequence of basalts at the free surface. However, the role of the associated reverse to thrust faults in the formation of the anticlines has been the subject of some debate. *Bentley* [1977] suggests that the basalts of the plateau were folded as well as faulted into anticlinal ridges and concludes that they are faulted drape folds generated by vertical movement of narrow basement blocks on high-angle reverse faults. *Bruhn* [1981] proposes a fault ramp-flexure mechanism involving a décollement near the base of the basalts to account for the geometry of the ridges. *Bentley* [1982] proposes that the anticlinal ridges are drag folds resulting from drag on interbasalt and subbasalt detachments or décollements [see *Campbell and Bentley*, 1981].

Price [1982] interprets the anticlinal ridges to be the results

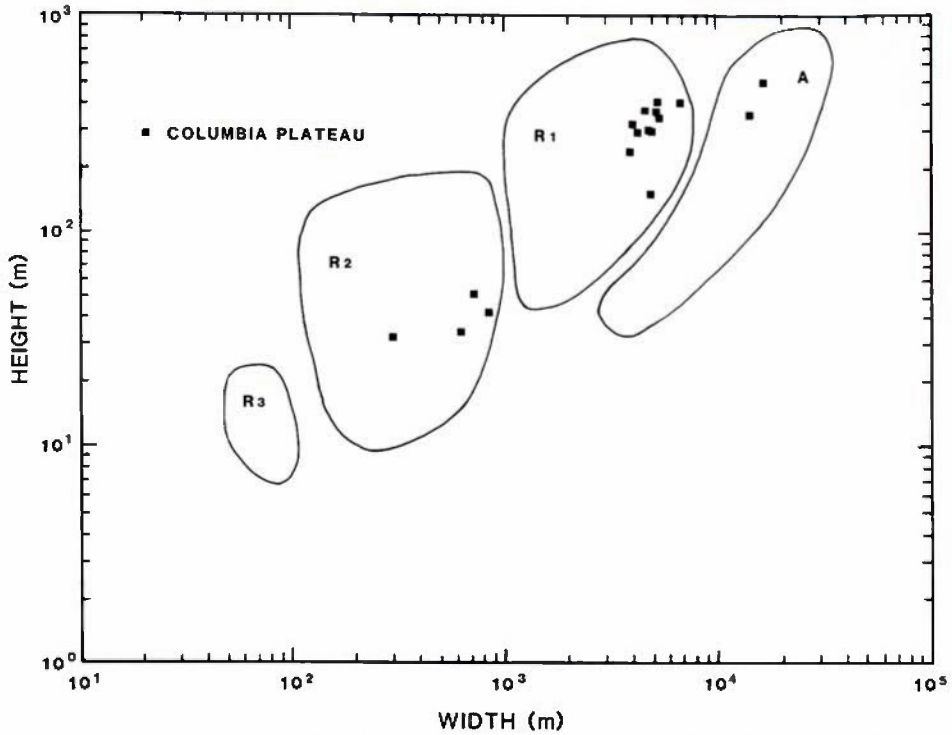

Fig. 9. Log-log plot of height versus width of 17 structures in the Yakima Fold Belt of the Columbia Plateau. The fields are defined by the planetary ridge and arch data shown in Figure 1.

of buckling developed over shallow detachments in the basalt sequence eventually followed by thrust faulting. Faulting is generated when the magnitude of the horizontal shortening is greater than can be accommodated by the concentric fold geometry. *Reidel* [1984] suggests that buckling (which may or may not be initiated by basement faulting) takes place until a maximum amplitude is reached, after which faulting occurs in the core of the fold at depth. Subsequent deformation occurs by faulting and folding. Based on the models of *Price* [1982] and *Reidel* [1984], faulting of the basalts postdates folding. If the anticlinal ridges of the Columbia Plateau are analogs to the ridges on the other terrestrial planets, then a similar origin for their formation may be appropriate.

Many of the terrestrial structures cited by *Plescia and Golombek* [1986] as analogs to planetary ridges are interpreted to be anticlines overlying a reverse or thrust fault. Based on these analogs, they suggest two kinematic models for the development of wrinkle ridges: (1) fault-bend folding in which a fold results from a thrust sheet translated over a nonplanar surface [*Suppe*, 1983] and (2) fault-propagation folding in which a fold develops over an upward propagating reverse fault that eventually reaches the surface. Thus the ridges on the Moon, Mars, and Mercury are interpreted to be folds with reverse to thrust faulting developed as a result of buckling (flexure-fracture; as proposed for the anticlinal ridges of the Columbia Plateau) or buckling the result of reverse or thrust faulting (fracture-flexure).

Estimates of Horizontal Shortening

Having established a basis for a structural interpretation of first-order ridges, it is relevant to consider the magnitude of the displacement (horizontal shortening) necessary to account for the topographic expression of the features. However, there are two problems with obtaining accurate estimates of the horizontal shortening in the ridged plains material of the Moon, Mars, and Mercury: (1) lack of high-resolution topographic data for the majority of the Moon and all of Mars and Mercury, and (2) the uncertainty in the subsurface structure (i.e., the extent of the involvement of reverse or thrust faults). In lieu of good topography the horizontal shortening can be estimated from measurements derived from remote sensing information on the morphology, dimensions, and spatial relationship of the ridges. This also assumes that all of the significant horizontal shortening is manifest in the topographic expression of the structure. If high-angle reverse faults are associated with the ridges, then the error in the estimated

TABLE 4. Dimensions of Features in Ridge Assemblages on the Columbia Plateau

Feature	$\bar{X}_w$	s_w	X_{max}–X_{min}	$\bar{X}_h$, m	s_h, m	X_{max}–X_{min}, m	n
Arches	15.6 km	1.0 km	17.0–14.2 km	437	54	513–360	2
Anticlinal ridges	4.9 km	0.7 km	6.9–3.9 km	322	68	412–153	11
Second-order ridges	619 m	156 m	834–300 m	40	6	51–33	4

$\bar{X}_w$, mean width; $\bar{X}_h$ mean height; s, standard deviation; range, X_{max}–X_{min}; and n, number of features. Measurements were made from U.S. Geological Survey topographic series maps of various scales (see the appendix).

Fig. 10. Enlargement of a portion of Figure 8 (Yakima Fold Belt). The Corral Creek (CC) and Grandview Butte (GB) anticlines are secondary folds that are morphologically and dimensionally similar to planetary second-order ridges (Landsat 4, frame ID 4009518173).

displacement obtained by restoring the topography to a planar surface should not be significant [see *Dahlstrom*, 1969]. If low-angle thrust faults are associated with the ridges, then the error in the estimated apparent displacement may be large. Given these considerations, the measure of strain employed is the unit elongation (normal strain) or, because the sign of the elongation is negative, the unit shortening. The unit shortening may be estimated assuming the ridge morphology can be geometrically approximated by a line in the form of either a plane triangle (symmetric form), a right triangle (asymmetric form), or a rectangle (box form). These geometric forms are representative of the shape of most of the ridges observed in this study. This also assumes that the deformation approximated by these forms involves translation alone (i.e., no distortion of the line). The unit shortening accomplished by the geometric forms as a function of amplification at a given width is shown in Figure 11. The estimates, using these forms, are upper and lower limits of the unit shortening assuming, as in the case of the Columbia Plateau, that the anticlinal ridges are separated by broad, largely undeformed synclines. The unit shortening is given by

$$\varepsilon = (l_d - l_u)/l_u \tag{1}$$

where ε is the unit shortening, l_d is line length of the deformed state, and l_u is the undeformed line length or the length necessary to restore the topography to a planar surface [see *Lia et al.*, 1978]. In this geometric analysis, $l_d = w$, where w is the width of the structure and thus the unit shortening is determined over the width of the ridge alone. The undeformed line length l_u for the symmetric form is given by

$$l_u = 2[(\tfrac{1}{2}w)^2 + h^2]^{1/2} \tag{2}$$

where h is the height or amplitude of the structure. For the asymmetric form, the line length is given by

$$l_u = [w^2 + h^2]^{1/2} + h \tag{3}$$

and for the rectangular fold form by

$$l_u = 2h + w \tag{4}$$

Using the mean values for width and height for the first-order ridges of Mars, the Moon, and Mercury from Tables 1–3, the estimated unit shortening across the structures and the corresponding displacements for the symmetric, asymmetric, and box fold geometries are shown in Table 5.

Estimates of horizontal shortening across mare ridges and

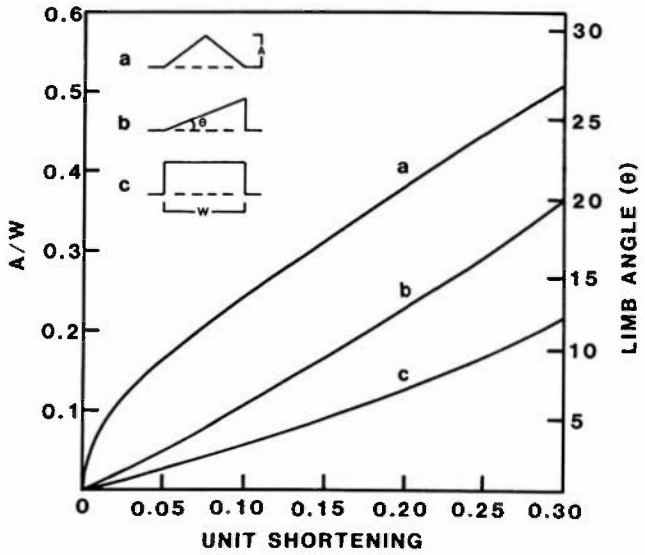

Fig. 11. The unit shortening as a function of the amplitude (A) to width (W) ratio of three fold forms: inset a, symmetric fold (plane triangle), inset b, asymmetric fold (right triangle), and inset c, box fold (rectangle). Method after *Currie et al.* [1962].

across Mare Serenitatis have been made by *Bryan* [1973], *Muehlberger* [1974], and *Maxwell et al.* [1975] using imagery and remote sensing data. *Bryan* [1973] estimates that a ridge 2–4 km wide and with a maximum elevation of 200 m would require a horizontal shortening of the order of 50 m across the structure. This corresponds to a unit shortening of about 0.01–0.03 (1–3% expressed as a percentage). *Bryan* [1973] also warns that intense overturning and thrusting would make these estimates misleadingly low. *Muehlberger* [1974] suggests that depending on the assumptions about the shape of the folded ridge, the strain represented by a mare ridge would range from a fraction of a percent to 5% across the structure. Using radar profiles obtained from the ALSE data, *Maxwell et al.* [1975] estimate a shortening of the order of 0.8% across the Serenitatis basin is necessary to account for the relief of mare ridges. The unit shortening over a first-order mare ridge of average dimensions ranges from about 0.008 to 0.11 or about 18–290 m of horizontal shortening across the structures (Table 5). Using a maximum horizontal shortening of 290 m per ridge and 214 m per mare arch, the estimated unit shortening across southern Serenitatis is approximately 0.006 (0.6%), in good agreement with the estimates of *Maxwell et al.* [1975].

Estimates of horizontal shortening based on detailed mapping have been made for the anticlinal ridges of the Columbia Plateau. *Bentley* [1982] concludes that along a 300-km section across the Columbia Plateau, 15 km of horizontal shortening is necessary to account for the more than 10 regularly spaced ridges. This amounts to between 1 and 2 km of horizontal shortening per structure. *Campbell and Bentley* [1981] estimate a maximum horizontal shortening of 1500 m over the Satus Park segment of Toppanish Ridge. *Price* [1982] estimates a total of 965 m of horizontal shortening over the Umtanum Ridge at Priest Rapids. This total is the sum of three separate components of displacement: (1) 540 m of horizontal shortening due to folding, (2) 175 m due to movement on the lower Umtanum fault, and (3) 250 m due to movement on upper Buck thrust (l_u = 3860 m, l_d = 2895 m). The unit shortening due to folding alone (i.e., less the components of displacement due to thrust faulting) is approximately 0.16 (l_u = 3435 m). *Reidel* [1984] estimates a maximum total horizontal shortening of 3000 m for Saddle Mountains ridge at Sentinel Gap. This total is also the sum of three displacements, 500 m due to folding and 2500 m due to movement on the lower and upper associated thrust faults (l_u = 8620 m, l_d = 5603 m). The unit shortening across the Saddle Mountains structure due to folding alone is about 0.08 (l_u = 6103 m).

The large difference in the unit shortening due to folding for the two anticlinal ridges can be explained by differences in fold geometry and the amplitude to width ratio (A/W). As would be expected, the unit shortening over an asymmetric fold at a given (A/W) is much less than that accommodated by a box fold (Figure 11). At the Sentinel Gap location the Saddle Mountains ridge has an asymmetric fold geometry [see *Reidel*, 1984, Figure 5*b*]. The fold geometry of the Umtanum Ridge at the Priest Rapids location is intermediate between an asymmetric fold and a box fold [*Price*, 1982]. Estimating an A/W of about 0.14 (400 m/2900 m) for the Umtanum at Priest Rapids, the unit shortening obtained for an intermediate asymmetric box fold geometry using equations (1), (3), and (4) (Figure 11) is approximately 0.17. Estimating an A/W of about 0.09 (500 m/5600 m) for the Saddle Mountains at Sentinel Gap, the expected unit shortening for an asymmetric geometry is of the order of 0.08.

The implications of the above observations for first-order ridges on the Moon, Mars, and Mercury are that (1) some degree of reverse or thrust faulting is likely in the formation of these structures, (2) some fraction of the total horizontal shortening may be due to displacement on reverse to thrust faults, and (3) estimates of the apparent unit shortening in some cases may be too low. The critical unit shortening (for a given A/W) that marks the onset of faulting is largely dependent on the fold geometry.

TABLE 5. Estimated Unit Shortening Across First-Order Ridges

	Symmetric		Asymmetric		Rectangular	
Planet	ε	u	ε	u	ε	u
Moon	0.008	18	0.06	150	0.11	290
Mars	0.03	81	0.12	352	0.20	664
Mercury	0.02	83	0.10	414	0.18	786

The unit shortening ε and corresponding displacement u (horizontal shortening) in meters were determined using equations (1)–(4) and mean dimensions for first-order ridges from Tables 1–3.

DISCUSSION

Nature of the Associated Faulting

It is clear from the preceding discussion that the nature and timing of faulting relative to folding is important in understanding the origin of both the anticlinal ridges of the Columbia Plateau and first-order ridges on the terrestrial planets. One line of evidence that is relevant to this question is the strain features commonly observed within and predicted for deformed materials in drape folds and thrust sheets (i.e., material deformed through fracture-flexure mechanisms).

Theoretical modeling by *Reches and Johnson* [1978], involving deformation of linear elastic or viscous multilayers, indicates that zones of layer-parallel shortening and extension will develop within all types of drape folds. *Freund* [1979] demonstrates that shortening associated with folds draped over reverse faults will progress from an early stage of layer-parallel shortening to predominantly layer-parallel extension.

Significant layer-parallel shortening and extension have been described in thrust plates and folds formed in conjunction with thrust faulting [*Price*, 1967; *Harris and Milici*, 1977; *Perry*, 1978; *Wojtal and Mitra*, 1986]. Layer-parallel extension faults are common on steeply dipping vertical or overturned beds of folds associated with thrust faults in the southern Rocky Mountains of Alberta [*Price*, 1967]. Evidence of layer-parallel shortening in the form of contraction faults producing shortening in the bedding plane is also common in folds associated with thrust faults [*Price*, 1967; *Harris and Milici*, 1977; *Wojtal and Mitra*, 1986].

Wiltschko [1979] modeled the deformation of a thrust plate on a nonplanar ramp using a plane strain linearly viscous model based on beam theory and employing the characteristics of the Pine Mountain thrust block. Stresses calculated for the thrust plate indicate that bending stresses are a significant portion of the total stresses and that zones of both normal and reverse faulting are predicted. *Wiltschko* [1979] argues that an element of material at the top or bottom of the thrust plate translated through the ramp will be subject to both normal and thrust fault regimes and concludes that the ramp portion of the thrust plate and the portion translated over the ramp would be expected to show complex faulting, particularly the outer surfaces where bending stresses are greatest.

In the Yakima folds, most of the strain is confined to the steeply dipping limbs, often characterized by layer parallel slip, layer-internal faulting and shattering [*Price*, 1982]. Layer-internal conjugate fault sets with minor displacements are common in both the steeply and gently dipping limbs of the anticlines. The crests of the anticlines are largely undeformed with little evidence of any layer-parallel extension. *Price* [1982] notes a distinct lack of significant layer-parallel extension in the exposed portions of the Umtanum Ridge. Minor graben (1- to 3-m vertical displacement) have been reported in the crest and hinge area of one segment of the Toppenish Ridge but are not found on any of the more than 50 segments with similar topography, stratigraphy, and structural settings in the fold belt [*Campbell and Bentley*, 1981].

Thus the deformed basalts within the anticlinal ridges of the Columbia Plateau lack strain features commonly associated with and predicted for drape folds or thrust plates translated through and over nonplanar fault ramps. Although it is not possible to characterize the strain features that may exist within first-order ridges on the other terrestrial planets in such detail, evidence for significant layer-parallel extension or complex faulting of the ridge crests may be detectable in high-resolution images of the Moon and Mars. Lineations have been observed on the crests of the Littrow ridge in eastern Serentitatis [*Howard and Muehlberger*, 1973; *Maxwell et al.*, 1975]. However, these lineations are rare and occur on a ridge associated with a mare ridge-highland scarp system (Figure 12) [see *Howard and Muehlberger*, 1973, Figure 31-37). These features are interpreted to be evidence of significant layer-parallel extension associated with the formation of the ridge by a fracture-flexure mechanism. This is consistent with the interpretation of *Howard and Muehlberger* [1973] and *Lucchitta* [1976] that the mare ridge-highland scarp systems are the result of reverse or thrust faulting.

Flexure-Fracture Mechanism

Two factors support a flexure-fracture mechanism for the formation of the anticlinal ridges of the Columbia Plateau and many of the first-order ridges on the Moon, Mars and Mercury: (1) the lack of strain features noted above and (2) the periodic nature of the anticlines and many first-order ridges. This periodic spacing must be accounted for in any kinematic or mechanical model. The periodic nature of the ridges is most easily explained by buckling [*Saunders and Gregory*, 1980; *Saunders et al.*, 1981; *Watters and Maxwell*, 1985*a*, *b*; *Anderson et al.*, 1987; *Watters*, 1987]. The periodic spacing of many of the anticlinal ridges of the Columbia and Tharsis plateaus may be explained by a layer instability resulting from a significant strength contrast between the basalts or ridged plains material and the substrate [*Watters*, 1987]. On the Columbia Plateau the basalts of the fold belt overlie several kilometers of weakly consolidated volcaniclastic sediments, while on the Tharsis Plateau the substrate is hypothesized to be a regolith consisting largely of impact breccia. Under a horizontal compressive load, the basalts buckle at a critical or dominant wavelength determined largely by the thickness of the strong layer (i.e., basalt sequence) and the modeled rheology [*Watters*, 1987]. The sediments or regolith must thicken locally under the folds to accommodate the structure. Thus the strength contrast between the materials controls where buckling will develop. This is evident on the Columbia Plateau by the lack of anticlines on the Palouse subprovince where the basalts overlie crystalline basement.

A significant regolith layer may also underlie mare basalts. Evidence of subsurface radar reflectors were detected in the ALSE data over Mare Serenitatis and Crisium. Reflectors at 1.6 and 1.4 km depths for Serenitatis and Crisium, respectively, are interpreted to be the results of deep-lying density inversions consisting of a regolith and/or pyroclastic layer [*Peeples et al.*, 1978; *Maxwell and Phillips*, 1978]. Thus a layer instability may also exist within lunar basins. In fact, given the crater production rates for the Moon and the other inner planets through geologic time [see *BVSP*, 1981] and the volume of ejecta expected in the formation of an impact basin, it is not unreasonable to assume a significant regolith underlies most of the smooth plains, intercrater plains, and basin fill material on Mars and Mercury.

Another factor that must be considered in models for the origin of these structures is the timing of deformation relative to the emplacement history of the flood volcanics. *Reidel* [1984] reports evidence of thinning of flows over the Saddle Mountains anticline. Some flows pinch out on the flanks or are embayed by the structure. He proposes that buckling was simultaneous with the emplacement of the oldest basalt flows and that the structural relief resulting from increased fold amplification was repeatedly buried by younger flows. Deformation therefore increases with depth and age. After the emplacement of the last flow, structural and topographic relief develop together.

Based on evidence of ponded flows on mare ridges, *Bryan* [1973] concludes that ridges formed contemporaneously with and following the emplacement of the basalts with the most intense deformation occurring after flow emplacement ceased.

Fig. 12. The Littrow ridge in the Taurus-Littrow region on the eastern margin of Mare Serenitatis. The lineations along the crest of the ridge (arrow) are interpreted to be evidence of significant layer-parallel extension.

Evidence of ponding of basalts by mare ridges has also been described by *Schaber* [1973*a*, *b*] and *Schaber et al.* [1976].

As mentioned previously, there is evidence of thinning of a mare unit on structural relief associated with a mare ridge assemblage in southeastern Serenitatis based on the stratigraphy inferred from subsurface reflectors detected in the ALSE data [see *Maxwell*, 1978, Figure 5]. However, *Sharpton and Head* [1982] suggest the unit thins on a premare volcanism topographic prominence which they attribute to a basin peak ring. Because the interpretation of the apparent thinning is dependent on the inferred stratigraphy, it is possible the unit thins on structural relief due to buckling over a major topographic deflection (peak ring) in the basin floor. Thus, as in the case of the Columbia Platcau, deformation may increase with depth and age of the basalts.

Based on the preceding discussion, the following kinematic models are submitted. Buckling begins early in the emplacement history of the basalt sequence in response to a horizontal compressive load coupled with layer instability between the basalts or smooth plains material and the underlying sediments or regolith. Concentric folds develop with a large component of simple shear strain, with some layer boundary slip. Structural relief is continuously buried by younger flows (Figure 13*a*, stage 1) until the emplacement of new flows cease. Now the entire sequence buckles but the radius of curvature of the basal layers is greater than the radius of curvature in

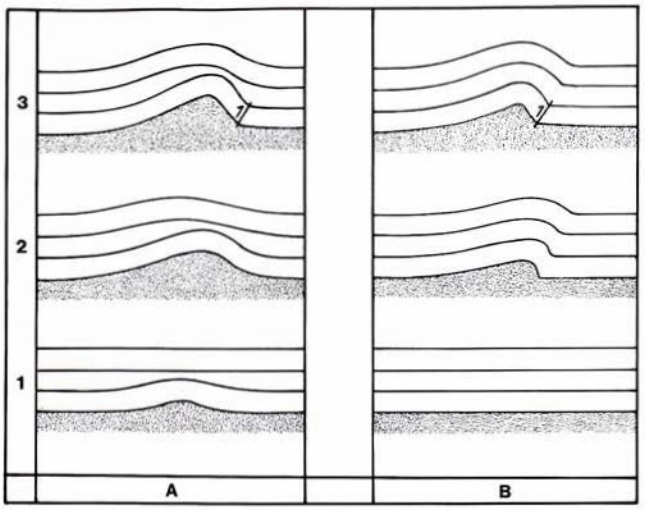

Fig. 13. Flexure-fracture mechanism for the formation of some of the first-order on the Moon, Mars, and Mercury and the anticlinal ridges of the Columbia Plateau. (*a*) Buckling begins early in the emplacement history, continuing after the last flow is emplaced. (*b*) Buckling begins after the entire sequence has been emplaced. As the folds begin to close, reverse to thrust faults develop at depth. Surface layers continue to deform by folding while reverse faults prograte up section and eventually reach the surface.

the upper layers (Figure 13*a*, stage 2). With increased amplification the fold closes at depth and reverse to thrust faulting occurs (Figure 3*a*, stage 3). Surface layers continue to deform by folding, while the reverse fault propagates up section and eventually reaches the free surface.

In an alternative model, deformation follows the emplacement of the entire sequence. Buckling begins in exactly the same way as in the preceding model (Figure 13*b*, stages 1 and 2). As amplification continues, the concentric fold closes at depth and reverse to thrust faults develop, as in the previous model (Figure 13*b*, stage 3).

It should be noted that these models are not intended to explain (1) mare ridge-highland scarp systems and (2) the ridges described by *Lucchitta and Klockenbrink* [1981] as "anastomosing" that occur on Mars and Mercury, many of which have been clearly influenced by buried crater rims. However, these models are applicable to basin ridges whose periodic spacing may be influenced by buried peak rings that create deflections in the multilayer (basalts or volcanic plains sequence) prior to buckling. The origin of the associated members of the ridge assemblage (i.e., arches and second- and third-order ridges) will be the subject of a future paper.

SUMMARY

The structures within the wrinkle ridge assemblage are classified as either arches or ridges on the basis of morphology and ridges are subdivided onto first-, second-, or third-order ridges on the basis of dimensions. The ridge assemblages described in this study are known to occur in mare basalts on the Moon and in smooth plains material which may be flood volcanic in origin on Mars and Mercury. The anticlinal ridges of the Columbia Plateau are appropriate analogs to first-order ridges because (1) they are similar in morphology and dimensions, (2) they occur in multilayered continental flood basalts, (3) they have associated structures that are analogous to other members of the planetary ridge assemblage, and (4) they are coparallel and periodically spaced. If the anticlinal ridges of the Columbia Plateau are appropriate analogs, then tectonic interpretations for the ridges are supported. Thus the ridges described in this study are interpreted to be folds with reverse or thrust faulting developed as a result of buckling (flexure-fracture) or buckling due to reverse or thrust faulting (fracture-flexure).

Estimates of the maximum horizontal shortening across first-order ridges on the Moon, Mercury, and Mars is about 290, 790, and 660 m, respectively. Estimates of the horizontal shortening in the anticlinal ridges of the Columbia Plateau, based on field analysis, are of the order of 1–2 km per ridge but include displacements due to movement on associated reverse to thrust faults as well as folding. Therefore estimates for the unit shortening across ridges on the Moon, Mercury, and Mars may be too low if significant horizontal displacements have occurred by movement on thrust faults.

The deformed basalts within the anticlinal ridges of the Columbia Plateau lack strain features commonly associated with and predicted for thrust plates translated through and over a nonplanar fault ramps or drape folds (i.e., significant layer-parallel extension and shortening). High-resolution images of the Moon and Mars reveal evidence of significant layer-parallel extension in only one ridge associated with a mare ridge-highland scarp system. The proposed flexure-fracture mechanism involves buckling in response to a horizontal compressive load coupled with a layer instability between the basalts or smooth plains material and the underlying sediments or regolith. Concentric folds develop with a large component of simple shear strain. With increased amplification, folds close and reverse to thrust faulting occurs.

APPENDIX: METHODS USED TO OBTAIN MEASUREMENTS

The height and width of 185 structures classified as members of wrinkle ridge assemblages on the Moon, Mars, and Mercury and 17 analogous structures on the Columbia Plateau in the northwestern United States were determined based on roughly 900 measurements. In order to avoid error that might be introduced by measuring superposed structures in the wrinkle ridge assemblage (i.e., determining the dimensions of a ridge superposed on an arch), only isolated features were measured. Widths were measured from (1) topographic profiles obtained from Lunar Topographic Orthophotomaps (LTOs) and U.S. Geological Survey (USGS) topographic maps, and (2) medium- to high-resolution images (images showing details from 500 to 10 m). Heights were measured from (1) topographic profiles and (2) shadow measurements obtained from medium- to high-resolution images with low incident angles ($\leq 20°$). Each dimension obtained was the average of a minimum of two measurements regardless of the method.

Measurements From Topographic Profiles

Topographic profiles were constructed perpendicular to the trend of the feature. The lateral limits of the feature were determined using major inflection points in the profile and checked by comparison with rectified images. Heights were measured by taking the difference between the maximum elevation on the profile and the average elevation level beyond the major inflection points marking the lateral limits of the feature. Sources of error in this method arise from factors such as (1) loss of detail due to the contour interval and (2) vertical

TABLE A1. Sampling Locations

Feature	Location
Moon	
Oceanus Procellarum	10°N, 50°W
Mare Cognitum	10°S, 25°W
Mare Imbrium	25°N, 20°W
Mare Serenitatis	25°N, 20°E
Mars	
Chryse Planitia	20°N, 50°W
Coprates	20°S, 70°W
Eridania	35°S, 120°E
Hellas Planitia	45°S, 70°E
Hesperia Planum	20°S, 110°E
Lunae Planum	10°N, 65°W
Schiaparelli	3°S, 16°E
Syrtis Major Planum	10°N, 70°E
Terra Sabaea	5°S, 27°E
Mercury	
Caloris Planitia	30°N, 5°W
Budh Planitia	20°N, 30°E
Odin Planitia	23°N, 8°E
Tir Planitia	3°N, 5°E

and horizontal accuracy of the mapped elevations. This is particularly a problem with the LTOs where the vertical accuracy is of the order of tens of meters and the horizontal accuracy is of the order of hundreds of meters [see *Ravine and Grieve*, 1986].

Measurements From Images

The images used in obtaining the measures were acquired from conventional optical cameras (i.e., Apollo metric camera and panoramic camera) and electro-optical cameras (i.e., Mariner 10 and Viking orbiter vidicon and Landsat multispectral scanner). Horizontal scales for the conventional rectified images were determined directly from the characteristics of the optical system and the dimensions of the negative. Horizontal scales for the rectified electro-optical images, were calculated using published map scales (i.e., USGS 1:2,000,000 controlled photomosaics of Mars, USGS shaded relief maps of Mercury). Widths were measured after the apparent lateral limits of the feature were determined. Heights were calculated from shadow measurements and incident angles obtained from the engineering data. Shadows were measured along the projected solar azimuth. Sources of error in this method arise from (1) uncertainties in estimating the lateral limits of a feature due to lack of contrast or prominent shadows, (2) uncertainties in estimating the horizontal extent of the shadows, (3) distortions due to rectification errors, (4) inaccuracies in computing the horizontal scale, and (5) artifacts resulting from digital image processing that distorts true shadows (i.e., blemish removal, shading corrections).

Sampling Locations

Features in the wrinkle ridge assemblage were measured in a number of different regions on the Moon, Mars, and Mercury (see Table A1). The statistical sampling is, of course, limited to areas with either high resolution topographic coverage (i.e., 10- to 20-m contour interval) or appropriate imagery (i.e., medium- to high-resolution, low incident angle, well-defined shadows).

Acknowledgments. I thank Robert Bentley, Matthew Golombek, the Associate Editor, Ted Maxwell, and Steve Reidel for their reviews. I am indebted to Ted Maxwell for many useful discussions and comments related to this paper, and Steve Reidel for his guidance in the field and discussions concerning the anticlinal ridges of the Columbia Plateau. I thank Michael Tuttle, John Chadwick, and Michael Rourke for their assistance in data collection. I also thank Donna Slattery for typing the manuscript, Rose Aiello and Michael Tuttle for their assistance in preparing the figures, and Priscilla Strain for editing the manuscript. This research was supported by NASA grant NAGW-940.

REFERENCES

Anderson, J. L., M. H. Beeson, and T. L. Tolan, Tectonic evolution of the southwest Columbia Plateau (abstract), *Geol. Soc. Am. Abstr. Programs, 19*, 354, 1987.

Basaltic Volcanism Study Project *Basaltic Volcanism on the Terrestrial Planets*, 1286 pp., Pergamon, New York, 1981.

Bentley, R. D., Stratigraphy of the Yakima basalts and structural evolution of the Yakima Ridges in the western Columbia Plateau, in *Geology Excursions in the Pacific Northwest*, edited by E. H. Brown and R. C. Ellis, pp. 339–389, Western Washington University, Bellingham, 1977.

Bentley, R. D., Later Tertiary thin skin deformation of the Columbia Plateau, Washington-Oregon (abstract) *Eos Trans. AGU, 63*, 173, 1982.

Bentley, R. D., J. L. Anderson, N. P. Campbell, and D. A. Swanson, Stratigraphy and structure of the Yakima Reservation with emphasis on the Columbia River Basalt Group, *U.S. Geol. Surv. Open File Rep., 80-200*, 73, 1980.

Binder, A. B., Post-Imbrian global lunar tectonism: Evidence for an initially totally molten moon, *Moon Planets, 26*, 117–133, 1982.

Binder, A. B., and H.-C. Gunga, Yound thrust-fault scarps in the highlands: Evidence for an initially totally molten moon, *Icarus, 63*, 421–441, 1985.

Bruhn, R. L., Preliminary analysis of deformation in part of the Yakima Fold Belt—South central Washington, report prepared pp. 27, Wash. Public Power Supply Syst., Richland, 1981.

Bryan, W. B., Wrinkle-ridges as deformed surface crust on ponded mare lava, *Proc. Lunar Sci. Conf., 4th*, 93–106, 1973.

Bryan, W. B., and M. L. Adams, Some volcanic and structural features of Mare Serenitatis, Apollo 17 Preliminary Science Report, *NASA Spec. Publ., SP-330*, 30-9–30-12, 1973.

Campbell, N. P., and R. D. Bentley, Later Quaternary deformation of the Toppenish Ridge uplift in south-central Washington, *Geology, 9*, 519–524, 1981.

Carr, M. H., R. Greeley, K. R. Blasius, J. E. Guest, and J. B. Murray, Some Martian volcanic features as viewed from the Viking orbiter, *J. Geophys. Res., 82*, 3985–4015, 1977.

Colten, G. W., K. A. Howard, and H. J. Moore, Mare ridges and arches in southern Oceanus Procellarum, Apollo 16 Preliminary Science Report, *NASA Spec. Publ., SP-315*, 29-90–29-93, 1972.

Currie, J. B., H. W. Patnode, and R. P. Trump, Development of folds in sedimentary strata, *Geol. Soc. Am. Bull., 73*, 655–674, 1962.

Dahlstrom, C. D. A., Balanced cross sections, *Can. J. Earth Sci., 6*, 743–757, 1969.

Donath, F. A., Role of layering in geologic deformation, *Trans. N. Y. Acad. Sci., 24*, 236–249, 1962.

Donath, F. A., and R. B. Parker, Folds and folding, *Geol. Soc. Am. Bull., 75*, 45–62, 1964.

Fecht, K. R., Geology of the Gable Mountain-Gable Butte area, *Rep. RHO-BEI-LD-5*, Rockwell Hanford Oper., Richlands, Wash., 1978.

Freund, R., Progressive strain in beds of monoclinal flexures, *Geology, 7*, 269–271, 1979.

Greeley, R., and P. D. Spudis, Ridges in western Columbia Plateau, Washington-Analogs to mare-type ridges (abstract), *Lunar Planet. Sci., IX*, 411–412, 1978.

Greeley, R., E. Theilig, J. E. Guest, M. H. Carr, H. Masursky, and J. A. Cutts, Geology of Chryse Planitia, *J. Geophys. Res., 82*, 4039–4109, 1977.

Harding, T. P., Tectonic significance and hydrocarbon trapping consequences of sequential folding with San Andreas faulting, San Joaquin Valley, California, *Am. Assoc. Pet. Geol. Bull., 60*, 356–378, 1976.

Harris, L. D., and R. C. Milici, Characteristics of thin-skinned style of deformation in the southern Appalachians, and potential hydrocarbon traps, *U.S. Geol. Surv. Prof. Pap., 1018*, 40 pp., 1977.

Hartman, W. K., and C. A. Wood, Moon: Origin and evolution of multi-ring basins, *Moon*, *3*, 1971.

Head, J. W., Lunar volcanism in space and time, *Rev. Geophys.*, *14*, 265–300, 1976.

Hodges, C. A., Mare ridges and lava lakes, Apollo 17 Preliminary Science Report, *NASA Spec. Publ.*, *SP-330*, 31-12–31-21, 1973.

Howard, K. A., and W. R. Muehlberger, Lunar thrust faults in the Taurus-Littrow region, Apollo 17 Preliminary Science Report, *NASA Spec. Publ.*, *SP-330*, 31-32–31-25, 1973.

Lia, W. M., D. Rubin, and E. Krempl, *Introduction to Continuum Mechanics*, 310 pp., Pergamon, New York, 1978.

Lucchitta, B. K., Mare ridges and related highland scarps-results of vertical tectonism, *Proc. Lunar Science Conf.*, *7th*, 2761–2782, 1976.

Lucchitta, B. K., Topography, structure, and mare ridges in southern Mare Imbrium and northern Oceanus Procellarum, *Proc. Lunar Science Conf.*, *8th*, 2691–2703, 1977.

Lucchitta, B. K., and J. L. Klockenbrink, Ridges and scarps in the equatorial belt of Mars, *Moon Planets*, *24*, 415–429, 1981.

Malin, M. C., Surfaces of Mercury and the Moon: Effects of resolution and lighting conditions on the discrimination of volcanic features, *Proc. Lunar Planet. Sci. Conf.*, *9th*, 3395–3409, 1978.

Maxwell, T. A., Origin of multi-ring basin ridge systems: An upper limit to elastic deformation based on a finite-element model, *Proc. Lunar Planet. Sci. Conf.*, *9th*, 3541–3559, 1978.

Maxwell, T. A., Orientation and origin of ridges in the Lunae Palus-Coprates region of Mars, *Proc. Lunar Planet. Sci. Conf. 13th*, Part 1, *J. Geophys. Res.*, *87*, suppl., A97–A108, 1982.

Maxwell, T. A., and A. W. Gifford, Ridge system of Caloris: Comparison with lunar basins, *Proc. Lunar Planet. Sci. Conf.*, *11th*, 2447–2462, 1980.

Maxwell, T. A., and A. W. Gifford, Ridge patterns of large craters and basins on Mars (abstract), *Lunar Planet. Sci.*, *XII*, 673–675, 1981.

Maxwell, T. A., and R. J. Phillips, Stratigraphic correlation of the radar-detected subsurface interface in Mare Crisium, *Geophys. Res. Lett.*, *5*, 811–814, 1978.

Maxwell, T. A., F. El-Baz, and S. W. Ward, Distribution, morphology, and origin of ridges and arches in Mare Serenitatis, *Geol. Soc. Am. Bull.*, *86*, 1273–1278, 1975.

Mouginis-Mark, P. J., V. L. Sharpton, and B. R. Hawke, Shiaparelli basin, Mars: Morphology, tectonics and infilling history, *Proc. Lunar Planet. Sci.*, *12A*, 155–172, 1981.

Muehlberger, W. R., Structural history of southeastern Mare Serenitatis and adjacent highlands, *Proc. Lunar Sci. Conf.*, *5th*, 101–110, 1974.

Oberbeck, V. R., W. L. Quaide, R. E. Arvidson, and H. R. Aggarwal, Comparative studies of lunar, Martian and Mercurian craters and plains, *J. Geophys. Res.*, *82*, 1681–1698, 1977.

Peeples, W. J., R. W. Sill, T. W. May, S. H. Ward, R. J. Phillips, R. L. Jordan, E. A. Abott, and T. J. Killpack, Orbital radar evidence for lunar subsurface layering in Maria Serenitatis and Crisium, *J. Geophys. Res.*, *83*, 3459–3468, 1978.

Perry, W. J., Jr., Sequential deformation in the central Appalachians, *Am. J. Sci.*, *278*, 518–542, 1978.

Philip, H., and M. Meghraoui, Structural analysis and interpretation of the surface deformation of the El Asnam earthquake of October 10, 1980, *Tectonics*, *2*, 17–49, 1983.

Plescia, J. B., and M. P. Golombek, Origin of planetary wrinkle ridges based on the study of terrestrial analogs, *Geol. Soc. Am. Bull.*, *97*, 1289–1299, 1986.

Price, E. H., Structural geometry, strain distribution, and tectonic evolution of Umtanum Ridge at Priest Rapids, and a comparison with other selected localities within Yakima fold structures, south-central Washington, Ph.D. dissertation, Wash. State Univ., Pullman, 1982.

Price, R. A., The tectonic significance of mesoscopic subfabrics in the southern Rocky Mountains of Alberta and British Columbia, *Can. J. Earth Sci.*, *4*, 39–70, 1967.

Raitala, J., Terra scarps indicating youngest terra faults on the Moon, *Earth Moon Planets*, *31*, 63–74, 1984.

Ramsay, J. G., *Folding and Fracturing of Rocks*, 568 pp., McGraw-Hill, New York, 1967.

Ravine, M. E., and R. A. F. Grieve, An analysis of morphologic variation in simple lunar craters, *Proc. Lunar Planet. Sci. Conf. 17th*, Part 1, *J. Geophys. Res.*, *91*, Suppl., E75–E83, 1986.

Reches, Z., and A. M. Johnson, Development of monoclines, part II, Theoretical analysis of monoclines, *Mem. Geol. Soc. Am.*, *151*, 273–311, 1978.

Reidel, S. P., Stratigraphy and petrogenesis of the Grande Ronde Basalts in the lower Salmon and adjacent Snake River Canyons, *Rep. RHO-SA-62*, Rockwell Hanford Oper., Richland, Wash., 1978.

Reidel, S. P., The Saddle Mountains: The evolution of an anticline in the Yakima fold belt, *Am. J. Sci.*, *284*, 942–978, 1984.

Reidel, S. P., and K. R. Fecht, The Huntzinger flow: Evidence of surface mixing of the Columbia River Basalt and its petrographic implications, *Geol. Soc. Am. Bull.*, *98*, 664–677, 1987.

Reidel, S. P., K. R. Fecht, and R. W. Cross, Constraints on tectonic models for the Columbia Plateau from age and growth rates of Yakima folds, in *Proceedings of 33rd Alaska Science Conference*, p. 131, Arctic Division, American Association for the Advancement of Science, Washington, D. C., 1982.

Reidel, S. P., G. R. Scott, D. R. Bazard, R. W. Cross, and B. Dick, Post-12 million year clockwise rotation in the central Columbia Plateau, Washington, *Tectonics*, *3*, 251–273, 1984.

Saunders, R. S., and T. E. Gregory, Tectonic implications of Martian ridges plains (abstract), Reports of Planetary Geology Program, 1980, *NASA Tech. Memo.*, *TM82385*, 93–94, 1980.

Saunders, R. S., T. G. Bills, and L. Johansen, The ridged plains of Mars (abstract), *Lunar Planet. Sci.*, *XII*, 924–925, 1981.

Schaber, G. G., Eratosthenian volcanism in Mare Imbrium: Sources of youngest lava flows, Apollo 17 Preliminary Science Report, *NASA Spec. Publ.*, *SP-330*, 31-22–31-25, 1973*a*.

Schaber, G. G., Lava flows in Mare Imbrium: Geologic evolution from Apollo orbital photography, *Proc. Lunar Sci. Conf.*, *4th*, 73–92, 1973*b*.

Schaber, G. G., Syrtis Major: A low-relief volcanic shield, *J. Geophys. Res.*, *87*, 9852–9866, 1982.

Schaber, G. G., J. M. Boyce, and H. J. Moore, The scarcity of mappable flow lobes on the lunar maria: Unique morphology of the Imbrium flows, *Proc. Lunar Sci. Conf.*, *7th*, 2783–2800, 1976.

Scott, D. H., Small structures of the Taurus-Littrow region, Apollo 17 Preliminary Sci. Report, *NASA Spec. Publ.*, *SP-330*, 31-25–31-28, 1973.

Scott, D. H., and M. H. Carr, Geologic map of Mars, *U.S. Geol. Surv. Misc. Invest. Map*, *I-803*, 1978.

Scott, D. H., and K. L. Tanaka, Geologic map of the western equatorial region of Mars, *U.S. Geol. Surv., Map*, *I-1802-A*, 1986.

Sharpton, V. L., and J. W. Head, The origin of mare ridges: Evidence from basalt stratigraphy and substructure in Mare Serenitatis (abstract), *Lunar Planet. Sci.*, *XII*, 961–963, 1981.

Sharpton, V. L., and J. W. Head, Stratigraphy and structural evolution of southern Mare Serenitatis: A reinterpretation based on Apollo Lunar Sounder Experiment data, *J. Geophys. Res.*, *87*, 10,983–10,998, 1982.

Strom, R. G., Lunar mare ridges, rings and volcanic ring complexes, *Mod. Geol.*, *2*, 133–157, 1972.

Strom, R. G., N. J. Trask, and J. E. Guest, Tectonism and volcanism on Mercury, *J. Geophys. Res.*, *80*, 2478–2507, 1975.

Suppe, J., Geometry and kinematics of fault-bed folding, *Am. J. Sci.*, *283*, 684–721, 1983.

Tjia, H. D., Lunar wrinkle ridges indicative of strike-slip faulting, *Geol. Soc. Am. Bull.*, *81*, 3095–3100, 1970.

Tolan, T. L., S. P. Reidel, M. H. Beeson, J. L. Anderson, K. R. Fecht, and D. A. Swanson, Revisions to the areal extent and volume of the Columbia River Basalt Group (CRBG) (abstract), *Geol. Soc. Am. Abstr. Programs*, *19*, 458, 1987.

Trask, N. J., and J. E. Guest, Preliminary geologic terrain map of Mercury, *J. Geophys. Res.*, *80*, 2461–2477, 1975.

Trask, N. J., and R. G. Strom, Additional evidence of mercurian volcanism, *Icarus*, *28*, 559–563, 1976.

Waters, A. C., Stratigraphy and lithologic variations in the Columbia River Basalt, *Am. J. Sci.*, *259*, 583–611, 1961.

Watters, T. R., The Columbia and Tharsis Plateaus, (abstract), *Geol. Soc. Am. Abstr. Programs*, *19*, 463, 1987.

Watters, T. R., and T. A. Maxwell, Crosscutting relations and relative ages of ridges and faults in the Tharsis region of Mars, *Icarus*, *56*, 278–298, 1983.

Watters, T. R., and T. A. Maxwell, Mechanisms of basalt-plains ridge formation (abstract), Reports of Planetary Geology Program 1984, *NASA Tech. Memo.*, *TM-87563*, 479–481, 1985*a*.

Watters, T. R., and T. A. Maxwell, Fold model for ridges of the Tharsis region of Mars (abstract), *Lunar Planet. Sci.*, *XVI*, 897–898, 1985*b*.

Watters, T. R., and T. A. Maxwell, Ridges of the Tharsis and Columbia Plateaus: A fold model (abstract), *Geol. Soc. Am., Abstr. Programs*, *17*, 745, 1985*c*.

Watters, T. R., and T. A. Maxwell, Orientation, relative age, and

extent of the Tharsis Plateau ridge system, *J. Geophys. Res.*, *91*, 8113–8125, 1986.

Whitaker, E. A., The surface of the Moon, in The nature of lunar surface, in *Proceedings of the 1965 IAU-NASA Symposium*, edited by W. N. Hess, D. H. Menzel, and J. A. O'Keefe, pp. 79–98, Johns Hopkins Press, Baltimore, Md., 1966.

Wilhelms, D. E., Mercury volcanism questioned, *Icarus*, *28*, 551–558, 1976.

Wiltschko, D. V., A mechanical model for thrust sheet deformation at a ramp, *J. Geophys. Res.*, *84*, 1091–1104, 1979.

Wojtal, S., and G. Mitra, Strain hardening and strain softening in fault zones from foreland thrusts, *Geol. Soc. Am. Bull.*, *97*, 674–687, 1986.

Yielding, G., J. A. Jackson, G. C. P. King, H. Sinvhal, C. Vita-Finzi, and R. M. Wood, Relations between surface deformation, fault (Algeria) earthquake of 10 October 1980, *Earth Planet. Sci. Lett.*, *56*, 287–304, 1981.

Young, R. A., W. J. Brennan, R. W. Wolfe, and P. J. Nichols, Volcanism in the lunar maria, Apollo 17 Preliminary Science Report, *NASA Spec. Publ.*, *SP-330*, 31-1–31-11, 1973.

T. R. Watters, Center for Earth and Planetary Studies, National Air and Space Museum, Room 3101B, Smithsonian Institution, Washington, DC 20560.

(Received April 15, 1987;
revised April 19, 1988;
accepted April 27, 1988.)